European Heart Journal (2000) **21,** 582–589
doi:10.1053/euhj.1999.1736, available online at http://www.idealibrary.com on IDEAL®

Cardiac rotation and relaxation in patients with aortic valve stenosis

E. Nagel, M. Stuber[1], B. Burkhard, S. E. Fischer[1], M. B. Scheidegger[1], P. Boesiger[1] and O. M. Hess

Cardiology, University Hospital Zurich and [1]Institute of Biomedical Engineering and Medical Informatics, University and Federal Institute of Technology, Zurich, Switzerland

Background Diastolic dysfunction with delayed relaxation and abnormal passive elastic properties has been described in patients with severe pressure overload hypertrophy. The purpose of this study was to evaluate the time course of rotational motion of the left ventricle in patients with aortic valve stenosis using myocardial tagging.

Methods Myocardial tagging is a non-invasive method based on magnetic resonance which makes it possible to label ('tag') specific myocardial regions. From the motion of the tag's cardiac rotation, radial displacement and translational motion can be determined. In 12 controls and 13 patients with severe aortic valve stenosis systolic and diastolic wall motion was assessed in an apical and basal short axis plane.

Results The normal left ventricle performs a systolic wringing motion around the ventricular long axis with clockwise rotation at the base ($-4{\cdot}4 \pm 1{\cdot}6°$) and counterclockwise rotation at the apex ($+6{\cdot}8 \pm 2{\cdot}5°$) when viewed from the apex. During early diastole an untwisting motion can be observed which precedes diastolic filling. In patients with aortic valve stenosis systolic rotation is reduced at the base ($-2{\cdot}4 \pm 2{\cdot}0°$; $P<0{\cdot}01$) but increased at the apex ($+12{\cdot}0 \pm 6{\cdot}0°$; $P<0{\cdot}05$). Diastolic untwisting is delayed and prolonged with a decrease in normalized rotation velocity ($-6{\cdot}9 \pm 1{\cdot}1\ s^{-1}$) when compared to controls ($-10{\cdot}7 \pm 2{\cdot}2\ s^{-1}$; $P<0{\cdot}001$). Maximal systolic torsion is $8{\cdot}0 \pm 2{\cdot}1°$ in controls and $14{\cdot}1 \pm 6{\cdot}4°$ ($P<0{\cdot}01$) in patients with aortic valve stenosis.

Conclusions Left ventricular pressure overload hypertrophy is associated with a reduction in basal and an increase in apical rotation resulting in increased torsion of the ventricle. Diastolic untwisting is delayed and prolonged. This may explain the occurrence of diastolic dysfunction in patients with severe pressure overload hypertrophy.
(Eur Heart J 2000; 21: 582–589)

Key Words: Myocardial tagging, left ventricular hypertrophy, diastolic dysfunction, aortic valve stenosis, cardiac torsion, magnetic resonance.

See page 512 for the Editorial comment on this article

Introduction

Diastolic dysfunction with delayed and incomplete relaxation has been reported to occur in patients with severe pressure overload hypertrophy[1–4]. According to the concept of Brutsaert *et al*.[5] diastolic dysfunction may precede the occurrence of systolic dysfunction in the development of myocardial failure. Diastolic function is predominantly altered by intracellular calcium overload, activation of the RAAS system[6,7] and/or an increase in collagen content with altered collagen architecture[8], and enhanced interstitial but also increased endocardial and perivascular fibrosis[8,9]. The diagnosis of diastolic dysfunction is most commonly achieved by assessing diastolic filling parameters using Doppler echocardiography[10]. These parameters depend, however, on several determinants such as heart rate, completeness and speed of relaxation, atrioventricular pressure gradient, afterload conditions, driving pressure, atrial and ventricular chamber properties, etc. The typical Doppler transmitral flow pattern with 'delayed' relaxation or a 'restrictive' flow pattern is unspecific and can be also found in patients with other cardiac diseases. Pressure–volume data allow differentiation between various mechanisms of left ventricular

Revision submitted 21 June 1999, and accepted 23 June 1999.

The study was supported by a grant of the Swiss Heart Foundation.

Correspondence: Eike Nagel, MD, Cardiology, German Heart Institute Berlin, Augustenburger Platz 1, D-13353 Berlin, Germany.

0195-668X/00/070582+08 $35.00/0

Table 1 Patient characteristics. Ejection fraction and wall thickness were determined with magnetic resonance tomography; valve area (Gorlin equation), aortic valve gradient (AVG) and peak systolic pressure (LVSP) were determined invasively. Mean ± 1 standard deviation and range are given

	n	Age (years)	Heart rate (beats . min^{-1})	Ejection fraction (%)	Wall thickness (mm)	Valve area (cm^2)	AVG (mmHg)	LVSP (mmHg)
Controls	12	29 ± 6 23–42	69 ± 5 54–76	61 ± 6 56–76	14·5 ± 1·3 11·1–16·1	—		—
Aortic valve stenosis	13	61 ± 12 38–78	71 ± 11 60–105	62 ± 9 53–84	20·7 ± 3·4 13·7–25·2	1 ± 0·34 0·32–1·5	65 ± 25 29–105	214 ± 27 179–256
Significance		$P<0·001$	ns	ns	$P<0·001$			

diastolic dysfunction such as prolonged relaxation, reduced filling rates and/or abnormal passive elastic properties[11].

With new technologies such as myocardial tagging based on magnetic resonance imaging, magnetization of the myocardium can be altered by spatial modulation[12] resulting in geometric patterns (= tags) which are fixed to the myocardium. With these tags specific myocardial regions can be non-invasively labelled with a star-like pattern[13], parallel lines[12] or a rectangular grid. From the deformation of the tags, regional three-dimensional wall motion including left ventricular rotation can be assessed[14–17]. Improvements in the initial technique[12] were achieved by using variable flip angles for image acquisition and by subtracting two measurements with complementary tagging signs (Complementary SPAtial Modulation of Magnetization=CSPAMM)[18,19] in combination with the use of a breath-holding scheme for reduction of motion artifacts. These refinements have led to a significant increase in tag persistence, which — in contrast to older tagging techniques — makes the analysis of one full cardiac cycle from the beginning of systole until late diastole with high temporal and spatial resolution possible. Image quality and measurement accuracy were further improved by the implementation of a slice-following technique, which permits the visualization of the same anatomical slice during cardiac contraction and relaxation independent of its through-plane motion.

The purpose of the present study was to determine cardiac rotation in patients with aortic valve stenosis in comparison to normal controls.

Methods

Patients

Twelve controls (four females, eight males, mean age 29 years, range 24–49 years) and 12 patients with severe aortic valve stenosis (two females, 10 males, mean age 61 years, range 38–73 years; aortic valve gradient of >75 mmHg or valve area below 0·5 cm^2 . m^{-2}) were included in the present analysis. The patient characteristics are listed in Table 1. Ten of the patients had symptoms, such as dyspnoea or angina, two patients had a previous syncope, in all patients signs of left ventricular hypertrophy were found in the resting ECG. In patients with severe symptoms aortic valve replacement was recommended.

Image acquisition

After obtaining informed consent all subjects were imaged with a conventional 1·5 Tesla magnetic resonance system (Gyroscan ACS II, Philips, Best, The Netherlands) in the prone position using a prototype cardiac surface coil. ECG and breathing motion were continuously recorded. After two short scans for the localization of the long axis, two short-axis planes (basal=2 cm below the valvular annulus, apical=3 cm above the left ventricular apex) were acquired and labelled with a rectangular grid (spacing=8 mm) using the CSPAMM technique[18,19]. The signal of the blood is suppressed by this technique and allows a clear definition of the endocardial border. Slice following was used to visualize the same myocardial regions throughout the cardiac cycle. A total of 16 images were sampled for each imaging plane beginning 50 ms after the R-wave and ending during the following end-diastole. Temporal resolution was 35 ms and spatial resolution 1·4 mm × 1·4 mm with a slice thickness of 6 mm at the apex and 8 mm at the base. To reduce motion artifacts a breath-hold scheme was used. The patient was asked to breathe regularly and stop briefly in expiration for image acquisition during every fourth or fifth heartbeat (TE=5·4 ms, TR=3200 ms). Examination time was approximately 8–12 min per slice.

Image analysis

The intersection points of the tagging lines were marked and traced semi-automatically in the different image planes using a custom written evaluation program (MACAVA) on a DEC alpha work station. Epi- and endocardial borders were defined manually in the first and calculated automatically in the following images using the motion of the grid crossing points.

End-diastole was defined as the first image after the R-wave, end-systole as the image with the smallest left ventricular area.

Definition of terms

Cardiac rotation (angular displacement around the centre of myocardial gravity when viewed from the apex) and fractional area change were determined in all patients. Torsion was calculated as the maximal rotation of the apex compared to the base at the same time point. Maximal systolic and diastolic rotation velocities were determined in all patients (=Vrot [° . s^{-1}]) and normalized for maximal rotation: Vnorm=Vrot/Rot_{max} [s^{-1}]. Time to peak rotation velocity (ms) was determined from the R-wave to maximal systolic rotation velocity and time to peak diastolic rotation from end-systole to maximal diastolic rotation velocity. Early and late diastolic filling (%) were defined as the amount of filling during the first and second half of diastole. For graphical display, times were normalized to % of the duration of systole.

Statistical analysis

Comparison between groups was performed with Student's t-test. Differences between different regions were tested by a paired Student's t-test. Linear regression analysis was performed to correlate different parameters. Mean values ± standard deviation are given in all tables and figures. A *P*-value of <0·05 was considered to be significant.

Results

A representative set of images is shown in Fig. 1 starting at end-diastole (upper left) and ending during the next end-diastole (lower right). Wall thickness was significantly increased in patients with aortic valve stenosis compared to controls ($P<0·001$). Ejection fraction and heart rate were similar in both groups (Table 1).

Systolic contraction

The normal left ventricle performs a systolic wringing motion with clockwise rotation at the base ($-4·36 \pm 1·6°$) and counterclockwise rotation at the apex ($+6·8 \pm 2·5°$) (Fig. 2) as seen from the apex. Systolic rotation at the apex occurs predominantly during isovolumic contraction in normal controls (Fig. 3) with no or only minimal rotation during systolic ejection. In patients with aortic valve stenosis, basal rotation is reduced ($-2·4 \pm 2·0°$, $P<0·01$) (Fig. 2(a)) but apical rotation is significantly increased and delayed as compared to the normal controls ($+12·0 \pm 6·0°$, $P<0·05$) (Fig. 2(b)). Torsion is significantly increased in patients with aortic valve stenosis ($14·1 \pm 6·4°$) when compared to controls ($8·0 \pm 2·1°$, $P<0·01$) (Fig. 2(c)). These numbers are smaller than the addition of apical and basal rotation as maximal apical rotation occurred earlier than maximal basal rotation. The time until peak rotation velocity is reached is normal in patients with pressure overload hypertrophy during systole ($37·2 \pm 19·6$ vs $34·4 \pm 14·1$, ns) (Fig. 4).

Diastolic relaxation and filling

During isovolumic relaxation an untwisting motion is observed in controls which is directed opposite to systolic rotation. Thus, diastolic rotation is counterclockwise at the base and clockwise at the apex. Diastolic rotation occurs predominantly during isovolumic relaxation with minimal rotation during filling. The apical rotation left ventricular area loop for controls and patients with aortic valve stenosis is shown in Fig. 3. In pressure overload hypertrophy not only systolic rotation but also diastolic untwisting is delayed and occurs simultaneously with left ventricular filling, resulting in a reduction in the rotation left ventricular area loop.

Time to peak diastolic rotation velocity was increased in patients with aortic valve stenosis when compared with controls ($103·1 \pm 28·2$ vs $56·0 \pm 24·5$, $P<0·0005$) (Fig. 4). A linear correlation between diastolic rotation velocity and maximal rotation existed for controls and patients with aortic valve stenosis (Fig. 5); however, the slope between rotation velocity and rotation was much flatter for patients with aortic valve stenosis in comparison to controls, due to a reduced peak normalized rotation velocity ($-6·9 \pm 1·1\ s^{-1}$ in patients with pressure overload hypertrophy vs $-10·7 \pm 2·2\ s^{-1}$ in controls, $P<0·001$).

Diastolic filling was delayed in patients with aortic valve stenosis with a significant reduction in early diastolic filling ($42 \pm 17\%$ vs $66 \pm 9\%$, $P<0·05$) but a significant increase in late diastolic filling when compared with controls. There was linear correlation between early diastolic filling and peak normalized rotation velocity (r=0·79).

Discussion

Cardiac torsion was described for the first time in the 1960s and 1970s in transplant recipients[20,21] using intramyocardial markers which had been implanted into the midmyocardium during open heart surgery. More recently, cardiac rotation and relaxation have been studied with echocardiography using echodense crystals implanted in the subendocardium with specifically designed catheters[22]. These authors described a twisting motion of the left ventricle with angular displacement (=torsion) of the apex relative to the base. However, these markers cannot be precisely located and have to be implanted by catheter techniques or surgically. The implantation of the markers may cause local scarring

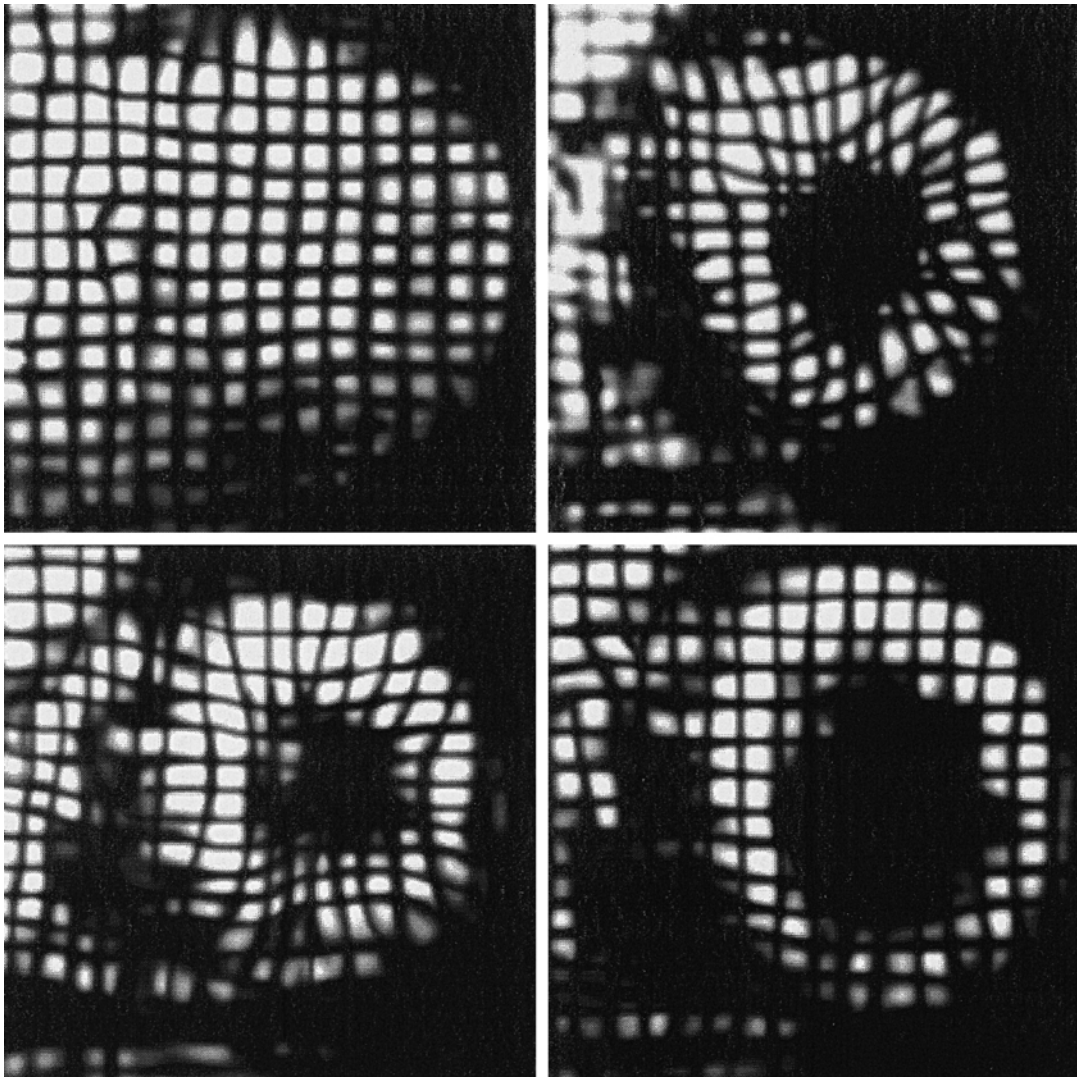

Figure 1 **A series of four out of 16 phases of the left ventricular apex in the short axis plane. The first end-diastolic frame is shown on the top left, an end-systolic frame on the top right, an early diastolic image on the bottom left and the end-diastolic frame of the next cardiac cycle on the lower right. Note the untwisting with minimal filling between the second and third image.**

and may induce abnormal wall motion not only due to the implantation procedure but also due to their weight and inertial properties. With new technologies, such as myocardial tagging the non-invasive analysis of regional cardiac motion is possible. From these measurements cardiac rotation and torsion have been determined in the normal human heart[23,24] as well as in patients with hypertrophic cardiomyopathy[14,15] and ischaemic heart disease[17].

The following observations have been made in the present study:

(1) When viewed from the apex, the normal left ventricle performs a systolic wringing motion with clockwise rotation at the base and counterclockwise rotation at the apex.

(2) In severe pressure overload hypertrophy basal (clockwise) rotation is reduced but apical (counterclockwise) rotation is increased resulting in an enhanced torsion of the left ventricle.

(3) Diastolic untwisting is delayed and peak normalized rotation velocity is reduced in aortic valve stenosis with an overlap of relaxation and early diastolic filling.

(4) Early diastolic filling is delayed in patients with aortic valve stenosis.

Pathophysiologic considerations

Systolic motion

In the normal left ventricle the clockwise rotation at the base and the counterclockwise rotation at the apex result

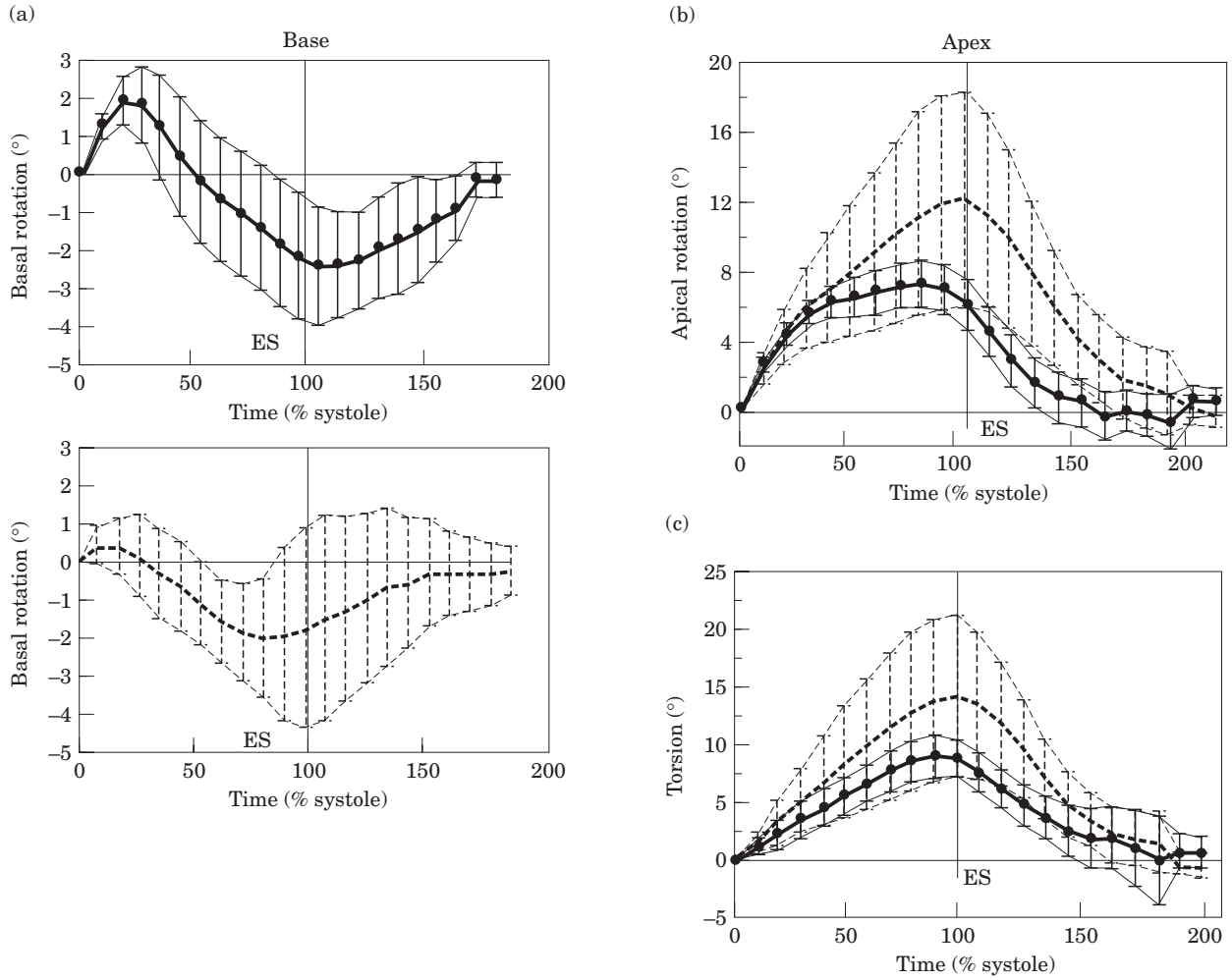

Figure 2 **Rotation–time plot at the base (a), at the apex (b) and torsion–time plot (c) in 12 controls and 13 patients with aortic valve stenosis. End-systole is indicated by the vertical line (ES). Basal rotation in aortic valve stenosis is reduced but enhanced at the apex, leading to enhanced torsion. —●—=controls; – – –=aortic stenosis.**

in a systolic wringing motion analogous to the wringing of a wet towel to squeeze the water out. From a theoretical standpoint, this wringing motion allows the ventricle to generate high intracavitary pressure with minimal shortening of the muscle fibres and, thus, minimal energy expenditure[25]. This characteristic motion of the left ventricle probably depends on the muscle fibre orientation, which has been described to be helical[26,27]. In the experimental animal it was shown that with an acute increase of afterload cardiac torsion as well as myocardial fibre shortening were significantly reduced, whereas torsion, but not shortening, persisted at isovolumic loading[28].

In aortic valve stenosis the physiological basal rotation of the left ventricle is reduced, which is consistent with the stiffening of the valvular plane and myocardial hypertrophy. However, apical rotation and torsion are increased, possibly due to a compensatory mechanism to increase intracavitary pressure.

Diastolic motion

In the normal left ventricle most diastolic untwisting occurs during isovolumic relaxation. Similar observations have been made in the experimental animal[29–32] and in humans[24]. A prolongation of the untwisting motion can be observed in patients with severe aortic valve stenosis with a reduction in peak normalized rotation velocity. This prolongation of diastolic untwisting may in part be responsible for the previously reported decrease in relaxation rate and diminished early diastolic filling velocity[33,34]. Although the extent of maximal rotation and the maximal rotation velocity is enhanced, the rotation velocity normalized for maximal rotation is reduced, probably due to muscle fibre hypertrophy and structural alterations of the myocardium with increased collagen content[8]. Thus, pressure overload hypertrophy is correlated with a prolongation of the untwisting process, a reduced rate of relaxation and a diminution of early diastolic filling. A linear

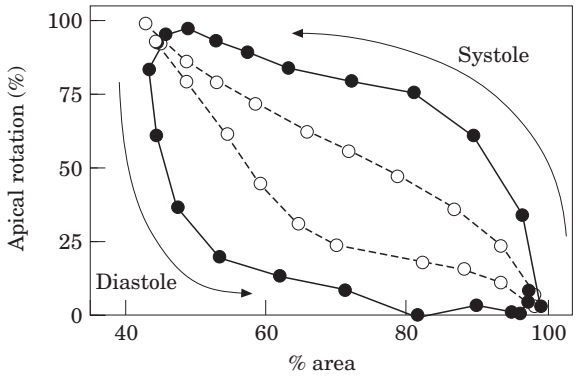

Figure 3 **Apical rotation left ventricular area loop in 12 controls (solid line) and 13 patients with aortic valve stenosis (broken line). The loops begin in the bottom right corner and are anticlockwise. Whereas rapid systolic rotation with minimal ejection followed by ejection with minimal rotation and a rapid diastolic untwisting with minimal filling followed by filling with minimal rotation can be observed in controls, ejection and rotation, as well as untwisting and filling occur simultaneously in patients with aortic valve stenosis.**

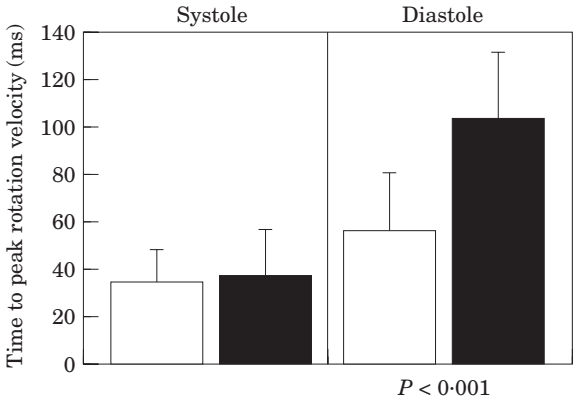

Figure 4 **Time to peak systolic (left) and diastolic (right) rotation velocity. The interval from end-diastole to peak systolic rotation is normal in aortic valve stenosis (■, n=13) but significantly prolonged from end-systole to peak diastolic rotation. □=controls, n=12.**

correlation was observed between early diastolic filling and normalized untwisting velocity, further underlining this interdependence. These changes may lead finally to diastolic dysfunction, which has been reported to occur frequently in patients with severe aortic valve stenosis[4]. A similar prolongation of diastolic untwisting has been reported in patients with hypertrophic cardiomyopathy[14], coronary artery disease and during acute rejection in heart transplant recipients[17,35–37].

Technical considerations

(1) Most previous studies have not used a correction algorithm for the translational motion of the heart. Thus, different regions of the left ventricle are imaged

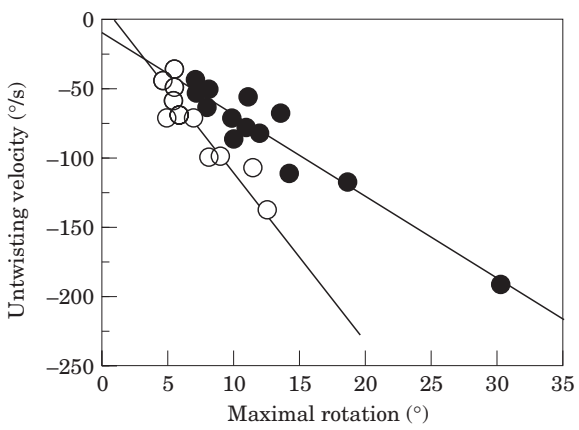

Figure 5 **Diastolic untwisting velocity vs maximal systolic rotation. The regression line in patients with aortic valve stenosis (●, n=13; r=0·95) has a flatter slope than in controls (○, n=13; r=0·95), indicating a reduced untwisting velocity for a given amplitude of systolic rotation.**

during cardiac contraction and relaxation, as seen with other tomographic techniques such as echocardiography, computed tomography, etc. In the current study, a slice following technique was used to eliminate the influence of the translational motion.

(2) In most previous analyses of cardiac motion with myocardial tagging, temporal resolution has been reported to be approximately 100 ms. Rapid motion components such as diastolic untwisting cannot be accurately studied with these techniques. In the present study, a temporal resolution of 35 ms was employed which makes the analysis of early diastolic events possible.

(3) Tag persistence is limited to approximately 400 ms with the conventional SPAMM technique and, thus, systolic rotation and diastolic untwisting cannot be evaluated during one single examination. The current CSPAMM technique has an increased tag contrast and tag persistence of more than 1000 ms and makes an accurate analysis of one complete cardiac cycle with high temporal and spatial resolution possible.

Limitations

The major limitation of the current study may be the comparison of healthy controls and patients from different age groups. It has been shown in previous studies, that ageing leads to a prolongation of diastolic filling and may even cause diastolic heart failure in otherwise healthy patients. However, there was a significant inverse correlation between left ventricular wall thickness and reduction of normalized untwisting velocity (r=0·82), but only a minimal correlation between age and normalized untwisting velocity within each group (r=0·31). Thus, the differences observed between the different groups are mainly due to pressure overload,

rather than the ageing itself, even though some influence cannot be excluded by our data.

A technical limitation is the long acquisition time of approximately 8–12 min which may be associated with motion artifacts. To overcome these problems a breath-holding scheme was used. Improvements in imaging technology help to circumvent these problems by single breath-hold sequences in combination with echo-planar imaging[38].

Filling and ejection were assessed from two short axis views only, rather than from a complete volume. However, the significant differences in diastolic filling between the groups observed from these two views correlate well with the results from the literature.

Clinical considerations

The increase in systolic apical rotation may be a compensatory mechanism to overcome increased afterload as cardiac rotation is an energy saving means of increasing intracavitary pressure with minimal shortening. However, this increase in systolic rotation cannot be adequately compensated for during diastolic untwisting. This part of the complex cardiac motion is delayed and prolonged, which may explain in part the occurrence of diastolic dysfunction in these patients. Diastolic untwisting may be a useful parameter to differentiate physiological hypertrophy, as found in athletes, from pathological hypertrophy such as found in aortic stenosis or hypertrophic cardiomyopathy.

References

[1] Hess OM, Schneider J, Koch R, Bamert C, Grimm J, Krayenbuehl HP. Diastolic function and myocardial structure in patients with myocardial hypertrophy. Special reference to normalized viscoelastic data. Circulation 1981; 63: 360–71.

[2] Topol EJ, Traill TA, Fortuin NJ. Hypertensive hypertrophic cardiomyopathy of the elderly. N Engl J Med 1985; 312: 277–83.

[3] Lorell BH, Grossman W. Cardiac hypertrophy: The consequences for diastole. J Am Coll Cardiol 1987; 9: 1189–93.

[4] Villari B, Hess OM, Kaufmann P, Krogmann ON, Grimm J, Krayenbuehl HP. Effect of aortic valve stenosis (pressure overload) and regurgitation (volume overload) on left ventricular systolic and diastolic function. Am J Cardiol 1992; 69: 927–34.

[5] Brutsaert D, Sys U, Gillebert T. Diastolic failure: pathophysiology and therapeutic implications. J Am Coll Cardiol 1993; 22: 318–25.

[6] Lorell BH. Diastolic dysfunction in pressure-overload hypertrophy and its modification by angiotensin II: current concepts. Basic Res Cardiol 1992; 2: 163–72.

[7] Apstein C, Morgan JP. Cellular mechanisms underlying left ventricular diastolic dysfunction. In: Gaasch WH, LeWinter MM, eds. Left ventricular diastolic dysfunction and heart failure. Philadelphia: Lea and Febiger, 1993: 3–24.

[8] Villari B, Campbell SE, Hess OM *et al.* Influence of collagen network on left ventricular systolic and diastolic function in aortic valve disease. J Am Coll Cardiol 1993; 22: 1477–84.

[9] Brilla CG, Maisch B, Weber KT. Myocardial collagen matrix remodelling in arterial hypertension. Eur Heart J 1992; 13 (Suppl D): 24–32.

[10] Spirito P, Muron BJ. Doppler echocardiography for assessing left ventricular diastolic dysfunction. Ann Intern Med 1988; 109: 122–6.

[11] Gaasch W, Blaustein A, Andrias C, Donahue AP, Avitall B. Myocardial relaxation. Part II: Hemodynamic determinants of rate of left ventricular isovolumic pressure decline. Am J Physiol 1980; 239: H1–H6.

[12] Axel L, Dougherty L. Heart wall motion: Improved method of spatial modulation of magnetization for MR imaging. Radiology 1989; 172: 349–50.

[13] Zerhouni EA, Parish DM, Rogers WJ, Yang A, Shapiro EP. Human heart: tagging with MR imaging — a method for noninvasive assessment of myocardial motion. Radiology 1988; 169: 59–63.

[14] Maier SE, Fischer SE, McKinnon GC, Hess OM, Krayenbuehl HP, Boesiger P. Evaluation of left ventricular segmental wall motion in hypertrophic cardiomyopathy with myocardial tagging. Circulation 1992; 86: 1919–28.

[15] Young AA, Kramer CM, Ferrari VA, Axel L, Reichek N. Three-dimensional left ventricular deformation in hypertrophic cardiomyopathy. Circulation 1994; 90: 854–67.

[16] de Roos A, van der Wall EE, Bruschke AV, van Voorthuisen AE. Magnetic resonance imaging in the diagnosis and evaluation of myocardial infarction. Magn Reson Q 1991; 7: 191–207.

[17] Nagel E, Stuber M, Matter C, Lakatos M, Boesiger P, Hess OM. Rotational and translational motion post myocardial infarction. J Cardiovasc Pharmacol 1996; 28: 31–5.

[18] Fischer SE, McKinnon GC, Maier SE, Boesiger P. Improved myocardial tagging contrast. Magn Reson Med 1993; 30: 191–200.

[19] Fischer SE, McKinnon GC, Scheidegger MB, Prins W, Meier D, Boesiger P. True myocardial motion tracking. Magn Reson Med 1994; 31: 401–13.

[20] Carlsson E, Milne ENC. Permanent implantation of endocardial tantalum screws: A new technique for functional studies of the heart in the experimental animal. J Can Assoc Radiol 1967; 19: 304.

[21] Ingels NB, Daughters GT 2nd, Stinson EB, Alderman EL. Measurement of midwall myocardial dynamics in intact man by radiography of surgically implanted markers. Circulation 1975; 52: 859–67.

[22] Myers JH, Stirling MC, Choy M, Buda AJ, Gallagher KP. Direct measurement of inner and outer wall thickening dynamics with epicardial echocardiography. Circulation 1986; 74: 164–72.

[23] Buchalter MB, Weiss JL, Rogers WJ *et al.* Noninvasive quantification of left ventricular rotational deformation in normal humans using magnetic resonance imaging myocardial tagging. Circulation 1990; 81: 1236–44.

[24] Rademakers FE, Buchalter MB, Rogers WJ *et al.* Dissociation between left ventricular untwisting and filling Accentuation by catecholamines. Circulation 1992; 85: 1572–81.

[25] Beyar R, Sideman S. Effect of the twisting motion on the nonuniformities of transmyocardial fiber mechanics and energy demand — a theoretical study. IEEE Trans Biomed Eng 1985; 32: 764–9.

[26] Lunkenheimer PP, Lunkenheimer A, Torrent-Guasp F. Der Aufbau des Myokardkörpers zu einem Schleifenkontinuum. In: Lunkenheimer PP, ed. Kardiodynamik: Wege zur strukturgerechten Analyse der Myokardfunktion. Beiträge zur Kardiologie, Band 33; Erlangen, Perimed Fachbuch Verlagsgesellschaft 1985.

[27] Streeter DD, Hanna WT. Engineering mechanics for successive states in canine left ventricular myocardium. II. Fiber angle and sarcomere length. Circ Res 1973; 23: 656–64.

[28] MacGowan GA, Burkhoff D, Rogers WJ *et al.* Effects of afterload on regional left ventricular torsion. Cardiovasc Res 1996; 31: 917–25.

[29] Arts T, Veenstra PC, Reneman RS. Epicardial deformation and left ventricular wall mechanisms during ejection in the dog. Am J Physiol 1982; 243: H379–90.

[30] Gibbons KC, Ter KH, Knudtson ML, Tyberg JV, Beyar R. An optical device to measure the dynamics of apex rotation of the left ventricle. Am J Physiol 1993; 265: H1444–9.
[31] Beyar R, Yin FC, Hausknecht M, Weisfeldt ML, Kass DA. Dependence of left ventricular twist-radial shortening relations on cardiac cycle phase. Am J Physiol 1989; 257: H1119–26.
[32] Hansen DE, Daughters GT 2nd, Alderman EL, Ingels NB Jr, Miller DC. Torsional deformation of the left ventricular midwall in human hearts with intramyocardial markers: regional heterogeneity and sensitivity to the inotropic effects of abrupt rate changes. Circ Res 1988; 62: 941–52.
[33] Murakami T, Hess OM, Gage JE, Grimm J, Krayenbuehl HP. Diastolic filling dynamics in patients with aortic stenosis. Circulation 1986; 73: 1162–74.
[34] Eichhorn P, Grimm J, Koch R, Hess OM, Carroll J, Krayenbuehl HP. Left ventricular relaxation in patients with left ventricular hypertrophy secondary to aortic valve disease. Circulation 1982; 65: 1395–404.
[35] Kroeker CA, Tyberg JV, Beyar R. Effects of ischemia on left ventricular apex rotation. An experimental study in anesthetized dogs. Circulation 1995; 92: 3539–48.
[36] Hansen DE, Daughters GT 2nd, Alderman EL, Stinson EB, Baldwin JC, Miller DC. Effect of acute human cardiac allograft rejection on left ventricular systolic torsion and diastolic recoil measured by intramyocardial markers. Circulation 1987; 76: 998–1008.
[37] Yun KL, Niczyporuk MA, Daughters GT 2nd, Ingels NB Jr, Stinson EB, Alderman EL, Hansen DE, Miller DC. Alterations in left ventricular diastolic twist mechanics during acute human cardiac allograft rejection. Circulation 1991; 83: 962–73.
[38] Tang C, McVeigh ER, Zerhouni EA. Multi-shot EPI for improvement of myocardial tag contrast: comparison with segmented SPGR. Magn Reson Med 1995; 33: 443–7.